Friction **9**(1): 61–74 (2021)
https://doi.org/10.1007/s40544-019-0324-0
ISSN 2223-7690
CN 10-1237/TH
RESEARCH ARTICLE

Effects of magnetic ionic liquid as a lubricant on the friction and wear behavior of a steel-steel sliding contact under elevated temperatures

Jiajia JIA[1], Guangbin YANG[1], Chunli ZHANG[1,2,*], Shengmao ZHANG[1,*], Yujuan ZHANG[1], Pingyu ZHANG[1]

[1] *Engineering Research Center for Nanomaterials, Henan University, Kaifeng 475004, China*

[2] *Institute of Pharmacy, Henan University, Kaifeng 475004, China*

Received: 28 February 2019 / Revised: 06 June 2019 / Accepted: 25 August 2019

Abstract: A magnetic ionic liquid (abridged as MIL) $[C_6mim]_5[Dy(SCN)_8]$ was prepared and used as the magnetic lubricant of a steel-steel sliding pair. The tribological properties of the as-prepared MIL were evaluated with a commercially obtained magnetic fluid lubricant (abridged as MF; the mixture of dioctyl sebacate and Fe_3O_4, denoted as DIOS-Fe_3O_4) as a control. The lubrication mechanisms of the two types of magnetic lubricants were discussed in relation to worn surface analyses by SEM-EDS, XPS, and profilometry, as well as measurement of the electric contact resistance of the rubbed steel surfaces. The results revealed that the MIL exhibits better friction-reducing and antiwear performances than the as-received MF under varying test temperatures and loads. This is because the MIL participates in tribochemical reactions during the sliding process, and forms a boundary lubrication film composed of Dy_2O_3, FeS, $FeSO_4$, nitrogen-containing organics, and thioether on the rubbed disk surface, thereby reducing the friction and wear of the frictional pair. However, the MF is unable to form a lubricating film on the surface of the rubbed steel at 25 °C, though it can form a boundary film consisting of Fe_3O_4 and a small amount of organics under high temperature. Furthermore, the excessive Fe_3O_4 particulates that accumulate in the sliding zone may lead to enhanced abrasive wear of the sliding pair.

Keywords: steel-steel sliding contact; magnetic ionic liquid; magnetic fluid; lubricant; tribological property; lubrication mechanism

1 Introduction

With the continuous progress of industrial technology, newly developed lubricants need to meet more and more stringent requirements for mechanical properties and lubricating performance [1–3]. Besides excellent load-bearing capacities, good friction-reducing, and antiwear abilities, they also need to exhibit self-repairing capabilities and environmental acceptance.

In this respect, magnetic lubricants as novel lubricants could be of special significance, because they can fill up the scratches and grooves on rubbed surfaces under an external magnetic field to achieve continuous lubrication, and they can counteract the effect of gravity and the centripetal force during the lubrication process, thereby preventing leakage and external pollution [4–6]. Currently, magnetic lubricants are often prepared by dispersing magnetic nanoparticles in conventional lubricants [7–9]. In recent years, magnetic fluids (MFs) as lubricants have been successfully applied to rolling bearings, sliding bearings, high-speed grinders, astronomical observation devices, and other mechanical equipments [10–12]. However, nanoparticles are thermodynamically unstable because of their high surface energy. In other words, they are susceptible to agglomeration and precipitation during long-term use or under varying environments (e.g., high temperature, high pressure), which hinders their practical

* Corresponding authors: Chunli ZHANG, E-mail: zclhd@henu.edu.cn; Shengmao ZHANG, E-mail: zsm@henu.edu.cn

application in engineering. Therefore, there is a need to develop new magnetic sealing and lubricating materials [13, 14].

Magnetic ionic liquids (MILs) composed of organic cations as well as inorganic or organic anions could be promising magnetic fluids, as the anion of MILs contains a magnetic center (with single electron organic free radical or metal ion complex) that can respond to an external magnetic field, thereby becoming magnetized [15–18]. However, MILs are essentially different from conventional magnetic lubricants used in tribology. On one hand, traditional magnetic lubricants are usually mixtures (lubricating base liquid + magnetic particles), but MILs are pure compounds rather than mixtures with multi-components, which means that MILs are homogeneous systems with thermodynamic stability and are free of aggregation, sedimentation, and phase separation. On the other hand, traditional MFs require a large amount of surfactant to achieve dispersion in the base fluid, which means that they often exhibit poor stability as compared with MILs. Moreover, traditional MFs exhibit undesired volatility and phase separation, but MILs often possess excellent high temperature stability and low (no) vapor pressure [19, 20]. Therefore, MILs as functionalized ionic liquids could be of special significance in tribology [21–23]. Driven by these perspectives, some researchers have been studying the synthesis of new MILs as well as investigating their physicochemical properties [24–26]. Now, the main problem with MILs as magnetic lubricants is that their magnetic properties are much poorer than those of conventional MFs. In other words, compared with traditional MFs, MILs often rely on a much stronger magnetic field to achieve magnetic manipulation [27]. Furthermore, few studies comparing the tribological properties of MILs and traditional MFs have been conducted.

Bombard et al. [28] prepared and investigated the tribological properties of ionic liquids, ionic liquid-based MFs (ionic liquids + carbonynyl iron particles), and PAO-based MF (PAO + carbonyl iron particles; PAO refers to poly-alpha olefin). They found that ionic liquids exhibit optimal antiwear effects for the steel-steel tribopair and polyformaldehyde-polyformaldehyde tribopair, and all ionic liquid-based MFs exhibit a much better friction-reducing ability than traditional PAO-based MFs. Shi et al. [29] synthesized an ionic liquid-based MF by modifying ferric oxide particles with a carboxyl functionalized ionic liquid, and suggested that the composite system could be applicable to extreme operating conditions requiring high temperature and low vapor pressure.

This research highlights the preparation of an MIL ($[C_6mim]_5[Dy(SCN)_8]$), where C_6mim refers to 1-hexyl-3-methylimidazolium. We also compare the antiwear mechanism and tribological properties of the as-prepared MIL with those of a traditional MF composed of DIOS and Fe_3O_4 (DIOS refers to dioctyl sebacate). Here, DIOS is used as the base stock for formulating the MFs, because, as an ideal carrier for preparing MFs widely used in mechanical sealing, lubrication, and other fields, it has excellent chemical stability and a good viscosity-temperature characteristic.

2 Experimental details

2.1 Preparation and characterization of MIL ($[C_6mim]_5[Dy(SCN)_8]$)

The MIL ($[C_6mim]_5[Dy(SCN)_8]$) was prepared according to Ref. [27]. Fourier transform infrared (FTIR) spectrum (Fig. S1) and element analysis results of the as-prepared MIL are shown in supporting information. The density of the MIL is 1.22 g/cm^3. The molecular structure of the as-prepared MIL is shown in Fig. 1. The as-prepared MIL, a light orange liquid, had a gram susceptibility of 32×10^{-6} emu/g. The mixture of dioctyl sebacate and Fe_3O_4 was purchased from Hu'nan Langrun Magnetoelectric Technology Company Limited (Zhuzhou, China). The as-received MF had a gram susceptibility of 50 emu/g; and Table 1 lists details about its appearance, density, particle size, and concentration. A thermal analyzer (METTLER TOLEDO DMA861e) was employed to evaluate the thermal stability of the MIL and MF (N_2 atmosphere; heating rate: 10 °C/min; temperature range: 25–800 °C). As shown in Fig. 2, the as-prepared MIL and the as-received MF undergo a mass loss of 5% at 243.7 and 230.0 °C, respectively, which indicates that they both exhibit good thermal stability. The viscosity of the samples was measured using a rotational rheometer (TA Instruments DHR2) at 25 °C. A conductivity instrument (SLDS, Nanjing Sangli Electronic Equipment Factory, Nanjing, China)

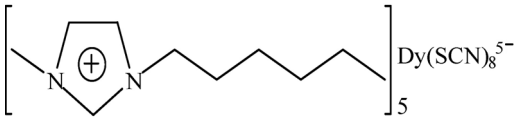

Fig. 1 Molecular structure of the MIL.

Table 1 Details about the appearance, density, particle size, and concentration of the MF.

Component	Particle size (nm)	Particle concentration (%)	Appearance	Density (g/cm^3, 25 °C)
DIOS-Fe_3O_4	20	20	Dark liquid	1.07

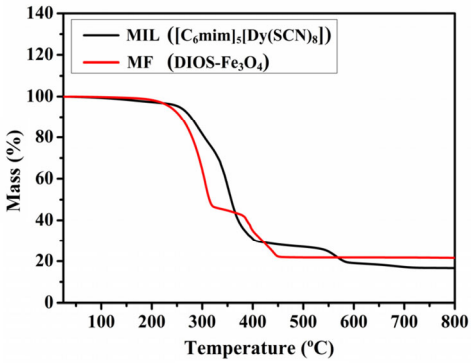

Fig. 2 TGA curves of the MIL and MF.

was employed to evaluate the conductivity of the MIL and MF at 25 °C. The results revealed that the base carrier DIOS and the as-received MF have no conductivity, while the as-prepared MIL has a conductivity of 135.84 μs/cm. The digital camera pictures of the MIL and MF are shown in Fig. 3, and it can be seen that the MIL is a homogeneous and transparent orange liquid.

Figure 4 shows the variations in the shear stress and viscosity of the MIL and MF with shear rate at

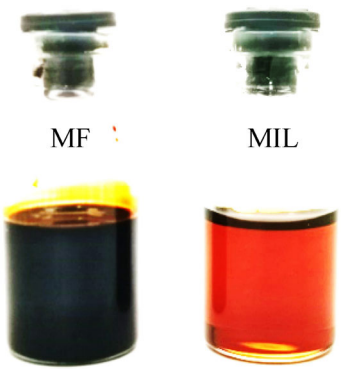

Fig. 3 Digital camera pictures of the MIL and MF.

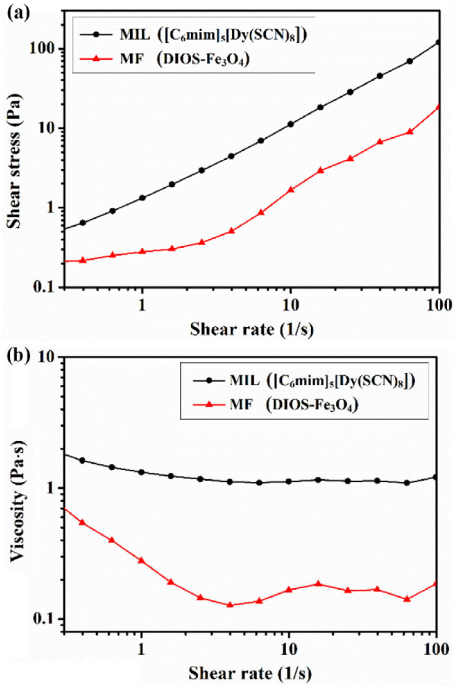

Fig. 4 Variations in (a) shear stress and (b) viscosity of the MIL and MF with shear rate at 25 °C.

25 °C. It can be seen that the as-prepared MIL has a higher viscosity than the MF in the selected shear rate range. Furthermore, the viscosity of the MF remarkably decreases with increasing shear rate, and it exhibits obvious shear-thinning characteristic in the early stage of shearing.

2.2 Friction and wear test

A high speed reciprocating friction and wear tester made by Huahui Instrument Technology Company Limited (Lanzhou, China) was employed to investigate the tribological properties of the as-prepared MIL and the as-received MF. The 316 steel ball (4 mm in diameter) and 304 non-magnetic steel disk (40 mm in diameter, 10 mm in thickness) comprised the ball-on-disk sliding pair. The schematic diagram of the tribopair is shown in Fig. 5. Prior to the sliding tests under various temperatures (25, 50, 100, and 150 °C), the lubricant was dropped into the contact zone. The test results were automatically logged to a computer linked to the test rig. Table 2 shows the sliding friction and wear test conditions at different temperatures.

2.3 Analysis of worn steel surfaces

A surface mapping profiler (Bruker Contour GT-K

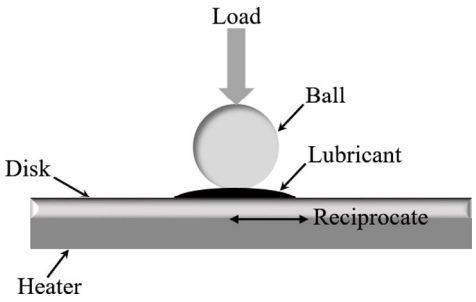

Fig. 5 Schematic diagram of the ball-on-disk sliding pair.

Table 2 Conditions for sliding friction and wear tests.

Parameter	Value
Oscillation frequency (Hz)	1
Normal load (N)	100, 200
Ball-on-disc sliding pair	316 steel ball / 304 steel disk
Stroke (mm)	5
Hardness (HV, ball / disk)	265/120
Surface roughness (nm, ball/disk)	200/20

Contour-K1) was employed to obtain the two-dimensional (2D) depth profiles and three-dimensional (3D) maps of wear scars. The morphology and element composition of the upper and lower worn surfaces were analyzed by field emission scanning electron microscopy (Gemini SEM 500). The chemical compositions of the worn surfaces were analyzed by X-ray photoelectron spectroscopy (XPS; Kratos AXIS ULTRA).

3 Results and discussion

3.1 Tribological behavior of a steel-steel contact lubricated by the MIL and MF

The coefficients of friction (abridged as COF) of the steel-steel sliding pair lubricated by the MIL and MF at 100 and 200 N under different testing temperatures are shown in Fig. 6. It can be seen that the MIL performs significantly better than the MF in reducing friction. In other words, the coefficients of friction of the steel-steel sliding pair lubricated by the MIL at 100 and 200 N at 25 ˚C are 0.17 and 0.18, respectively, much lower than those obtained under MF lubrication (0.27 and 0.26). As the temperature increases, the friction-reducing performance of the MIL varies slightly, but the coefficients of friction under MF lubrication remain high (e.g., 0.47 at 100 ˚C and 0.29 at 150 ˚C). This indicates

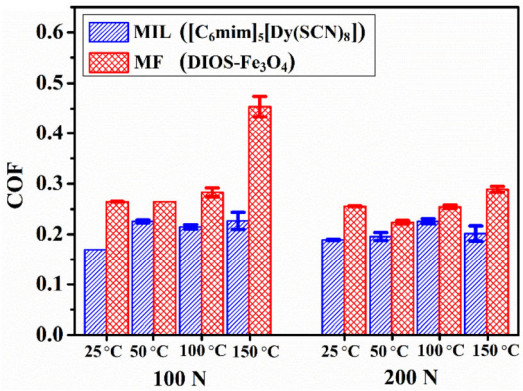

Fig. 6 Coefficients of friction of the steel-steel sliding pair lubricated by the MIL and MF at different temperatures (25, 50, 100, 150 ˚C) and loads (100 and 200 N).

that the as-prepared MIL as a magnetic lubricant for the steel-steel sliding pairs exhibits good friction-reducing and antiwear behavior from 25 to 150 ˚C.

The wear volumes of a steel-steel sliding contact lubricated by the MIL and MF at 100 and 200 N under different temperatures are shown in Fig. 7. The wear volume of a steel-steel sliding contact lubricated by the MIL under different loads rises slowly with increasing temperature, but the value for the steel-steel sliding contact lubricated by the MF under the same conditions tends to rise more quickly therewith.

This implies that the as-prepared MIL is advantageous over the as-received MF in reducing the wear of the steel-steel contact at different temperatures. In particular, the wear volume of the lower steel disk lubricated by the as-received MF tends to rise sharply when the temperature rises from 100 to 150 ˚C, regardless of the varying load. In other words, it

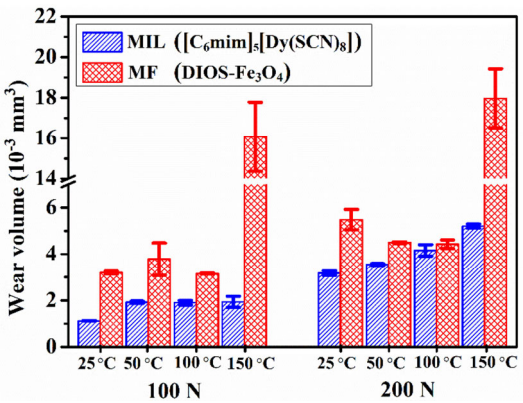

Fig. 7 Wear volumes of a steel-steel sliding contact lubricated by the MIL and MF at different temperatures (25, 50, 100, 150 ˚C) and loads (100 and 200 N).

increases from 3.2×10^{-3} to 16.1×10^{-3} mm^3 under 100 N and from 5.4×10^{-3} to 17.9×10^{-3} mm^3 under 200 N, which corresponds well with the poor antiwear behavior of the MF under elevated temperatures.

Figure 8 shows the variation curves of friction over time at different temperatures. It can be seen that, under MIL lubrication at 25 ℃, the initial coefficient of friction increases slightly from 0.17 to 0.18 when the normal load increases from 100 to 200 N. Under MF lubrication, however, the coefficient of friction is large and tends to fluctuate significantly, especially at 100 N (Fig. 8(a)). At other temperatures (Figs. 8(b)–8(d)), the coefficient of friction varies in a manner similar to that in Fig. 5(a); in general, the friction curve under MIL lubrication at different temperatures is lower and more stable than that under MF lubrication.

3.2 Analysis of the worn surface of a lower steel disk and upper steel ball

Figures 9 and 10 show the 3D wear scar maps and partial enlargement pictures of wear scars under the lubrication of the MIL and MF as well as 2D wear scar depth profiles at 100 N and different temperatures (25 and 150 ℃). The wear scars of the steel disk and ball lubricated by the MIL at different temperatures are much smoother than those under MF lubrication. Namely, there is a small amount of scratches and deep grooves on the worn surface under MF lubrication (Figs. 9(e) and 9(f)), and the depth and amount of the grooves on the wear scar tend to increase with increasing temperature (Figs. 10(e) and 10(f)). However, the wear scars of the steel disk and ball lubricated by the MIL, are much smaller than those lubricated by the MF and contain fewer scratches and grooves, as evidenced by relevant 2D depth profiles of the wear scars (Figs. 9(g), 9(h), 10(g), and 10(h)).

In particular, under high temperature conditions, a transfer film higher than the worn surface is formed on the worn surface of the upper steel ball under MF lubrication at elevated temperatures, as evidenced by the relevant 3D topography (Fig. 10(f)).

Figure 11 shows the SEM micrographs of worn disk surfaces under MF and MIL lubrication at 25 ℃ and 100 N. Under the MF lubrication, deep grooves and a large amount of wear debris are present on the worn surface of the steel disk (Figs. 11(a) and 11(b)). This indicates that the steel disk mainly undergoes abrasive damage under MF lubrication, which corresponds well with the 3D maps of the wear scars. This is because, during the sliding process, Fe_3O_4 particles enter the frictional contact area and participate in the friction and wear process, resulting in three body abrasions. Under MIL lubrication, the worn surface

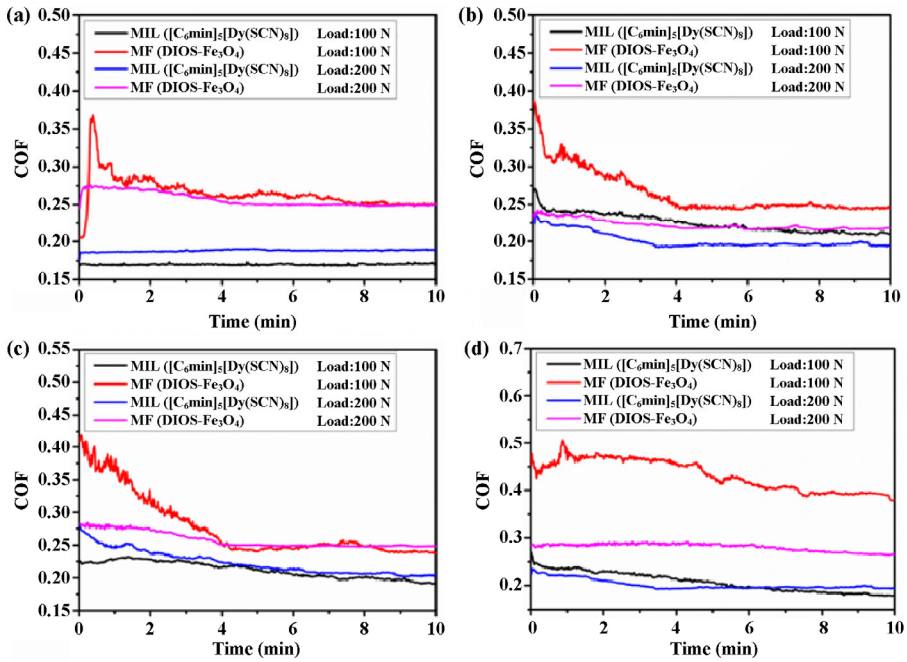

Fig. 8 Variation curves of friction with time: (a) 25, (b) 50, (c) 100, and (d) 150 ℃.

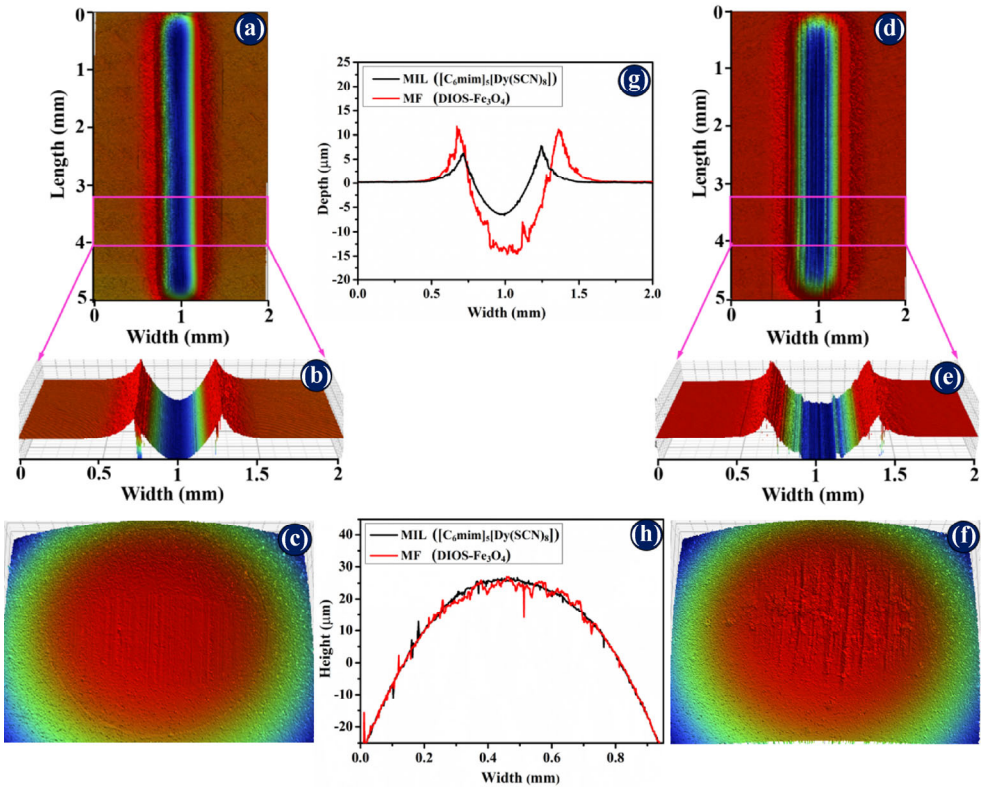

Fig. 9 3D images of wear scars and partially enlarged pictures of wear scars of a steel disk and upper steel ball lubricated by (a–c) the MIL and (d–f) MF, as well as (g, h) 2D contrast pictures of the wear scar depth profile at 100 N and 25 ˚C.

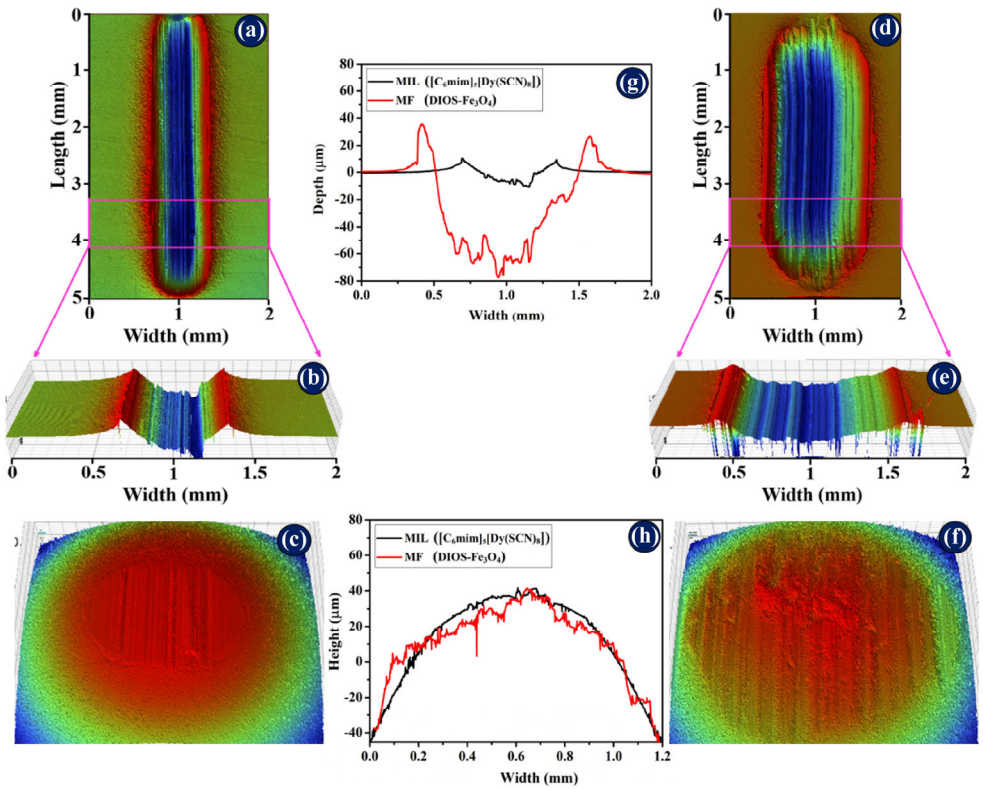

Fig. 10 3D images of wear scars and partially enlarged pictures of wear scars of a steel disk and upper steel ball lubricated by (a–c) the MIL and (d–f) MF, as well as (g, h) 2D wear scar depth profiles at 100 N and 150 ˚C.

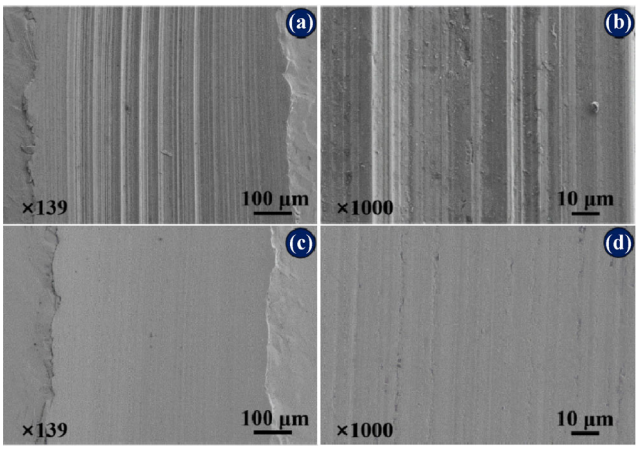

Fig. 11 SEM micrographs of the worn disk surfaces under (a, b) the MF and (c, d) MIL lubrication under 100 N and 25 ˚C.

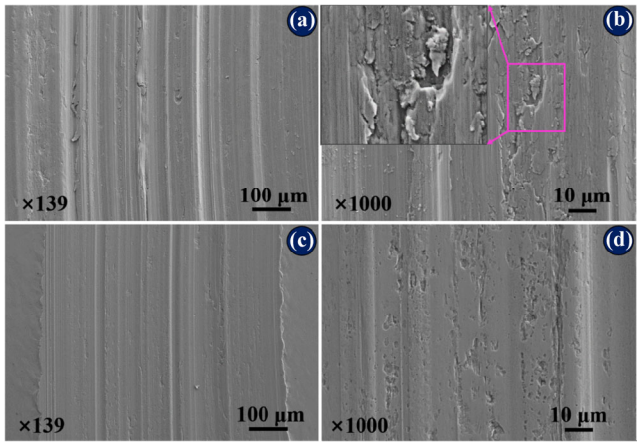

Fig. 12 SEM micrographs of worn disk surfaces under (a, b) the MF and (c, d) MIL lubrication under 100 N and 150 ˚C.

of the steel disk is smooth and shows almost no sign of friction-induced damage (Figs. 11(c) and 11(d)). This implies that the MIL exhibits favorable antiwear ability for the steel-steel sliding contact.

Figure 12 shows the SEM micrographs of worn disk surfaces under MF and MIL lubrication at 100 N and 150 ˚C. At a high temperature of 150 ˚C, grooves are formed on the worn surface lubricated with MIL (Figs. 12(c) and 12(d)), which indicates that the wear of the sliding contact is exacerbated at elevated temperatures. Under MF lubrication, the steel disk surface seems to undergo more serious abrasion damage at 150 than at 25 ˚C (Figs. 12(a) and 12(b)). As reported elsewhere, the MF particle tends to agglomerate during the friction process, thereby resulting in abrasive wear in association with scratches and grooves on the rubbed surfaces [30–32]. As the temperature rises, abrasive wear is exacerbated to result in increases in the depth and amount of the scratches and grooves. Furthermore, the phase equilibrium of the MF may be destroyed under elevated temperature, and the deposition of the nanoparticle on the friction contact area could be enhanced, thereby causing an increase in the wear volume.

The SEM micrographs and EDS analysis of worn surfaces under MIL lubrication at 100 N and 150 ˚C are shown in Fig. 13. Dy, S, and N are detected on the rubbed surfaces of the steel ball and disk; in particular, S is significantly enriched in the contact area of the sliding pair. This means that MIL as a lubricant can form a boundary lubrication film via adsorption and a chemical reaction. Besides, the worn steel surface under MIL lubrication seems to be quite smooth and contains no obvious grooves compared with the one lubricated with MF, which conforms well with the observation that the MIL exhibits better friction-reducing and antiwear performances for the steel-steel contact than the MF.

The SEM micrographs and EDS analysis of the worn surfaces under MF lubrication at 100 and 150 N are shown in Fig. 14. Together with the 3D topography of the upper steel ball (Fig. 10(f)), they indicate that a deposit layer is formed on the worn surface of the lower steel disk, while a transfer layer is formed on the worn surface of the upper steel ball (Figs. 14(a) and 14(b)). Corresponding EDS analysis indicates that the tribofilm contains a large amount of Fe and O, which implies that a thick tribofilm is formed on the rubbed surface of the steel disk after sliding at 150 ˚C. Along with destruction of the asperities under a normal load and shear force, the large wear debris is formed, thereby causing scratches and grooves on the rubbed steel surface; furthermore, an increase and fluctuation in the coefficient of friction is observed [33].

Under the ideal fluid lubrication condition, the electric contact resistance (abridged as ECR) between the sliding pair should tend to be infinite, as the frictional pair would be separated by a layer of lubricant. When the steel-steel sliding pair comes into direct contact after extended sliding, the electric resistance would become very small, owing to the metal-metal contact. Figure 15 shows the variation in the electric contact resistance of the tribopair lubricated by MIL and MF at different temperatures with sliding

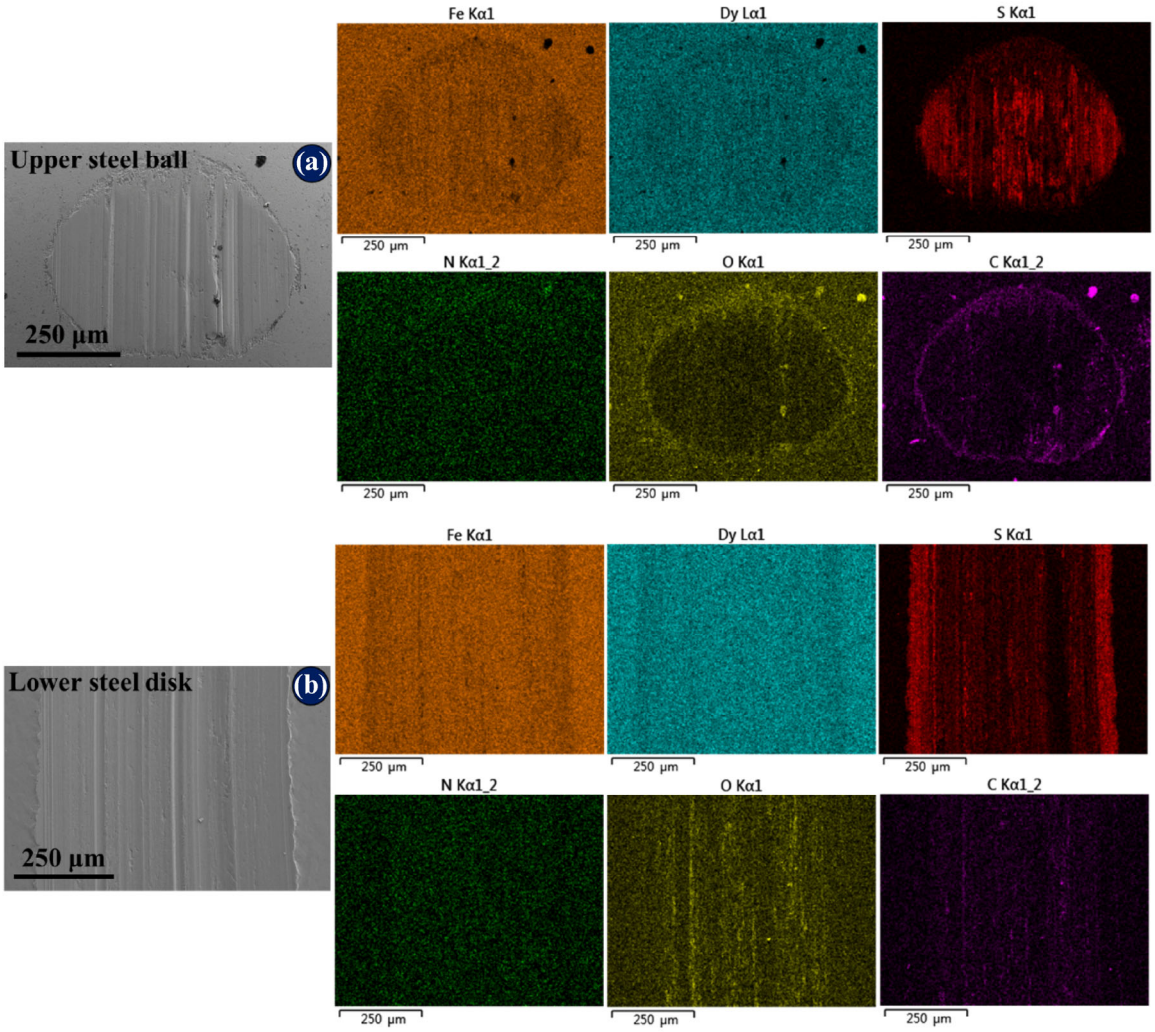

Fig. 13 SEM micrographs and EDS analysis of worn surfaces of an (a) upper steel ball and (b) lower steel disk under MIL lubrication at 100 N and 150 ℃.

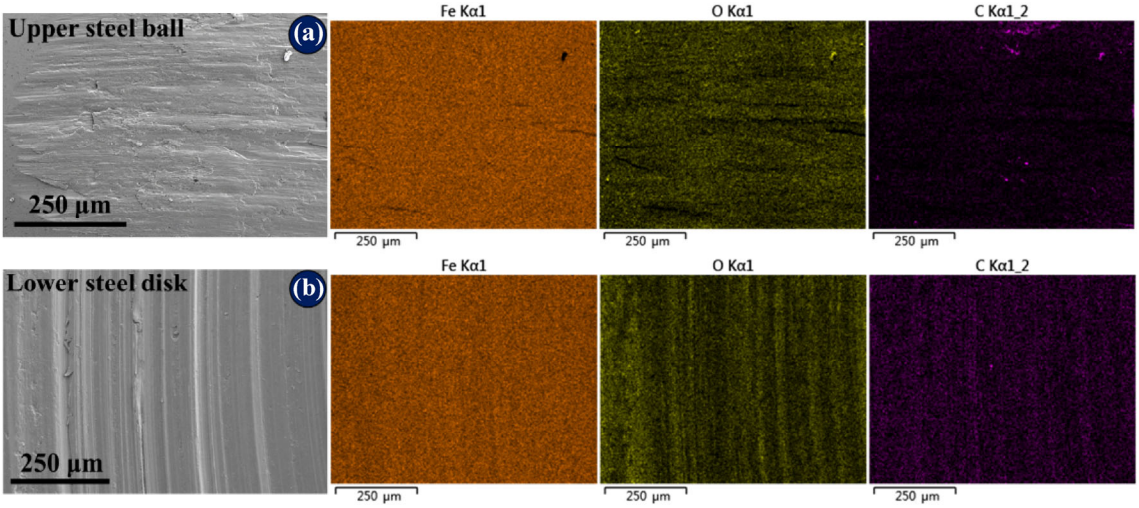

Fig. 14 SEM micrographs and EDS analysis of worn surfaces of an (a) upper steel ball and (b) lower steel disk under MF lubrication at 100 N and 150 ℃.

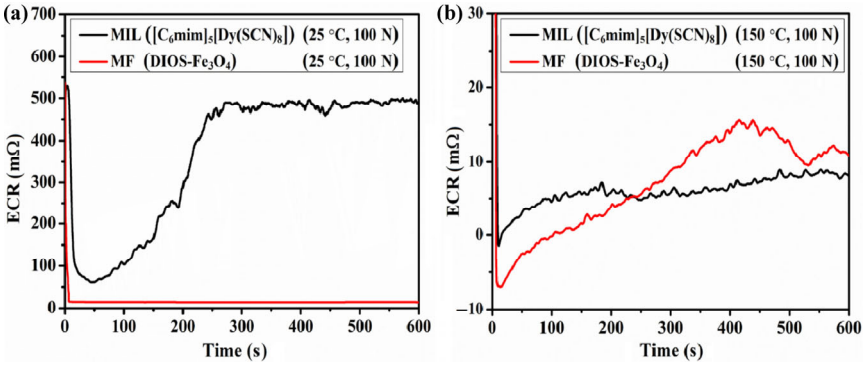

Fig. 15 Variation in the electric contact resistance of the sliding pair lubricated by MIL and MF versus time at (a) 25 and (b) 150 ℃.

time. Under MIL lubrication at 25 ℃, the electric contact resistance stays at a low level in the initial stage of rubbing (tens of second), and then it gradually increases with extending sliding time (Fig. 15(a)). After sliding for 250 s, the resistance value tends to be stable. This is because MIL can form an adsorption film on the rubbed surfaces of the frictional pair (supporting information, Fig. S2) to hinder its direct contact.

As the sliding time rises, a boundary lubrication film composed of an adsorption film and tribochemical reaction film is formed on the rubbed steel surface, thereby leading to a gradual increase in the electric contact resistance therewith. However, the MF can hardly form an effective boundary lubrication film at 25 ℃, and in this case, the electric contact resistance is almost zero owing to the direct contact between the steel-steel sliding pairs.

When the MIL is used as the lubricant at elevated temperature, the electric contact resistance of the steel-steel sliding pair reaches a relatively stable value after sliding for 100 s, but it stays at a lower level compared with the one at 25 ℃ (Fig. 15(b)). This could because it is more difficult for the adsorption film to form on the rubbed steel surface under an elevated temperature, and the tribochemical reaction mainly accounts for the formation of a boundary lubrication film thereon. As a result, the steel-steel sliding pair would have a greater opportunity to achieve direct contact under elevated temperatures, which results in significantly reduced electric contact resistance thereat. When the MF acts as the lubricant under a high temperature, the Fe_3O_4 particles can form a deposited layer on the rubbed surface of the frictional pair. As the friction process progresses, the thickness of the deposited layer increases, and the contact resistance also increases therewith. As Fe_3O_4 itself has a certain conductivity, the contact resistance value finally remains constant at approximately 10 mΩ.

To further explore the lubrication mechanism of MILs and MFs, we analyzed the chemical state of the worn surface elements by XPS (before performing XPS analysis, the steel disks were ultrasonically cleaned with ethanol and petroleum ether to remove any residual lubricant on the worn surfaces). Figure 16 shows the curve-fitted XPS spectra of the worn surface under MF at 150 ℃ and 100 N. The $Fe2p_{3/2}$ and $Fe2p_{1/2}$

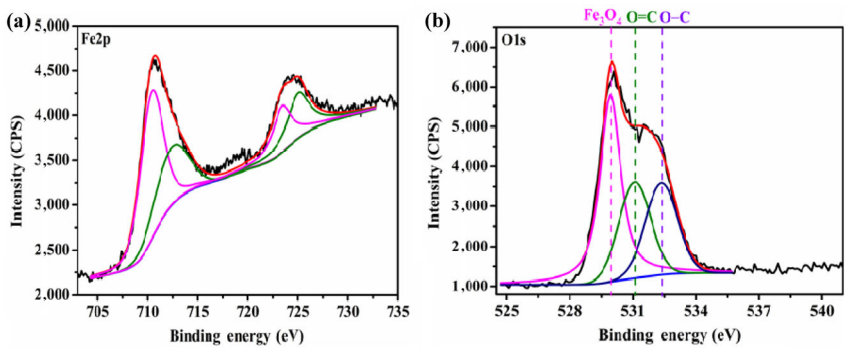

Fig. 16 Curved-fitted XPS spectra of worn steel surface under lubrication of MF at 150 ℃ and 100 N: (a) Fe2p and (b) O1s.

peaks at 710.6 and 724.1 eV are attributed to Fe_3O_4 [34]; in particular, the $Fe2p_{3/2}$ peak can be assigned to Fe^{2+} and Fe^{3+} species with a deconvoluted area ratio of 1:2, which is consistent with the stoichiometry of Fe_3O_4 [35, 36]. The O1s spectrum can be deconvoluted into three peaks at 529.6, 531.1, and 532.3 eV, and they are assigned to Fe_3O_4, C=O bond, and C-O bond, respectively [37, 38].

The curve-fitted XPS spectra of the worn surface under MIL lubrication at 150 ˚C and 100 N are shown in Fig. 17. The $Dy4d_{3/2}$ and $Dy4d_{5/2}$ peaks emerge at 153.2 and 156.7 eV, respectively, which is in agreement with the oxidation state of Dy_2O_3 [39, 40]. Three S2p peaks emerge at 161.9, 163.1, and 168.5 eV, respectively. The peak at 161.9 eV is combined with the Fe2p peak at 710.1 eV, corresponding to FeS [41, 42]. The S2p peak at 163.1 eV is attributed to the C–S–C bond [43]. The S2p peak at 168.5 eV, in association with the Fe2p peak at 713.2 eV and O1s peak at 532.4 eV, reveals the existence of $FeSO_4$ [41, 44]. The Fe2p peak at 711.2 eV and the O1s peak at 530.2 eV can be attributed to Fe_2O_3 [34, 41]. The N1s spectrum can be deconvoluted into three peaks centered at 398.4, 400.0, and 402.1 eV, and they can be assigned to the C–N bond, amide group, and N–O or N–N bond, respectively [45–47]. The O1s peak at 533.3 eV corresponds to ether-type oxygen produced under complex friction conditions [48].

The results of the XPS analysis of the worn surfaces indicate that, when an MF acts as a lubricant, a boundary film mainly composed of a Fe_3O_4 deposited layer (Fe2p 710.6 eV and O1s 529.7 eV) and a small amount of organics are formed on the worn steel disk surface. When an MIL is used as the lubricant, a tribochemical reaction film composed of Dy_2O_3 (Dy4d 153.2 and 156.7 eV, O1s 530.1 eV), FeS (Fe2p 710.1 eV, S2p 161.9 eV), $FeSO_4$ (Fe2p 713.2 eV, S2p 168.5 eV and O1s 523.4 eV), nitrogen containing organics, and a thioether compound is formed on the rubbed steel surface. In other words, under MIL lubrication, the frictional sliding process involves tribochemical reactions, which help to reduce friction and wear.

4 Conclusions

A novel magnetic ionic liquid $[C_6mim]_5[Dy(SCN)_8]$ is prepared and used as the magnetic lubricant of a steel-steel sliding tribo-pair. Comparative studies with a commercial mixture of dioctyl sebacate and Fe_3O_4 as a control indicate that the as-prepared MIL is superior to the MF in reducing the friction and wear of the ball-on-disk sliding contact, especially under an elevated temperature of 150 ˚C. This is because, as evidenced by SEM-EDS, XPS, profilometry analyses of the worn steel surfaces, and measurement of the electric contact

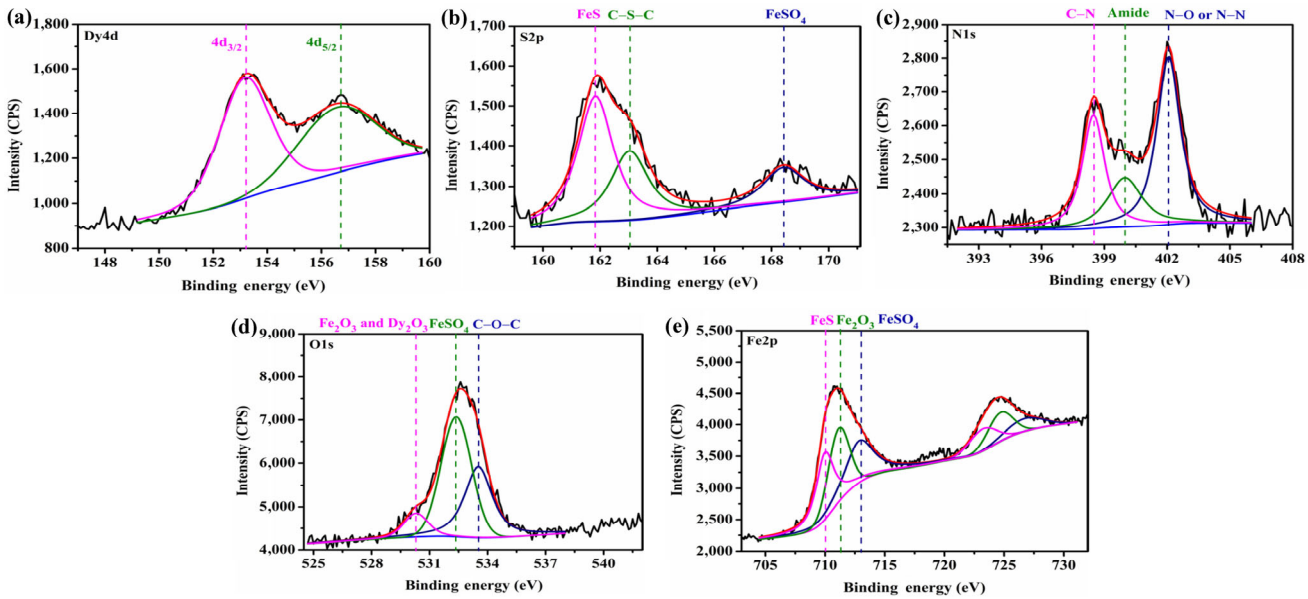

Fig. 17 Curve-fitted XPS spectra of the worn steel surface under MIL lubrication at 150 ˚C and 100 N: (a) Dy4d, (b) S2p, (c) N1s, (d) O1s, and (e) Fe2p.

resistance, the as-prepared MIL participates in tribochemical reactions in the sliding process to form a desired boundary lubrication film on the worn steel surfaces. In other words, the tribochemical reactions give rise to a boundary lubrication film composed of Dy_2O_3, FeS, $FeSO_4$, nitrogen-containing organics, and thioether on the worn area, which significantly reduces the friction and wear of the steel-steel tribo-pair. However, the commercial MF is unable to form a lubricating film on the rubbed steel surface under 25 ℃ conditions, though it can form a boundary film consisting of Fe_3O_4 and a small amount of organics under high temperatures. Even worse, the MF as the lubricant allows excessive Fe_3O_4 accumulate in the sliding zone, thereby enhancing abrasive wear of the steel-steel sliding contact. In summary, the as-prepared MIL could be a promising magnetic lubricant for the steel-steel sliding contact in a relatively wide range of temperatures (from 25 to 150 ℃).

Acknowledgements

We acknowledge the financial support provided by the National Natural Science Foundation of China (Grant Nos. 51605143, 21671053, 51775168, and 51875172) and the Scientific and Technological Innovation Team of Henan Province Universities (Grant No. 19IRTSTHN024).

Electronic Supplementary Material: Supplementary material is available in the online version of this article at https://doi.org/10.1007/s40544-019-0324-0.

References

[1] Lertola A C, Wang B C, Li L. Understanding the friction of nanometer-thick fluorinated ionic liquids. *Ind Eng Chem Res* **57**(34): 11681–11685 (2018)

[2] Bakhtiyarov S I, Kutelia E R, Siginer D A. Thermometric studies of newly developed nanolubricants. In *ASME 2016 International Mechanical Engineering Congress and Exposition*. Phoenix, Arizona, USA, 2016.

[3] Wong V W, Tung S C. Overview of automotive engine friction and reduction trends–Effects of surface, material, and lubricant-additive technologies. *Friction* **4**(1): 1–28 (2016)

[4] Weng H C, Chen L Y. A hydrostatic bearing test system for measuring bearing load using magnetic-fluid lubricants. *J Nanosci Nanotechnol* **16**(5): 5218–5221 (2016)

[5] Wang L J, Guo C W, Ryuichiro Y, Wu Y. Tribological properties of Mn–Zn–Fe magnetic fluids under magnetic field. *Tribol Int* **42**(6): 792–797 (2009)

[6] Zin V, Agresti F, Barison S, Litti L, Fedele L, Meneghetti M, Fabrizio M. Effect of external magnetic field on tribological properties of goethite (a-FeOOH) based nanofluids. *Tribol Int* **127**: 341–350 (2018)

[7] Zhang P, Dong Y Z, Choi H J, Lee C H. Tribological and rheological tests of core-shell typed carbonyl iron/polystyrene particle-based magnetorheological fluid. *J Ind Eng Chem* **68**: 342–349 (2018)

[8] Trivedi K, Parekh K, Upadhyay R V. Nanolubricant: Magnetic nanoparticle based. *Mater Res Express* **4**(11): 114003 (2017)

[9] Laurent S, Dutz S, Häfeli U O, Mahmoudi M. Magnetic fluid hyperthermia: Focus on superparamagnetic iron oxide nanoparticles. *Adv Colloid Interface Sci* **166**(1–2): 8–23 (2011)

[10] Hu Z D, Wang Z, Huang W, Wang X L. Supporting and friction properties of magnetic fluids bearings. *Tribol Int* **130**: 334–338 (2019)

[11] Wang Z Z, Li D C, Zhou J. Non-uniform distribution of magnetic fluid in multistage magnetic fluid seals. *J Magn* **22**(2): 299–305 (2017)

[12] Kandasamy G, Sudame A, Luthra T, Saini K, Maity D. Functionalized hydrophilic superparamagnetic iron oxide nanoparticles for magnetic fluid hyperthermia application in liver cancer treatment. *ACS Omega* **3**(4): 3991–4005 (2018)

[13] Medvedeva I, Uimin M, Yermakov A, Mysik A, Byzov I,

Nabokova T, Gaviko V, Shchegoleva N, Zhakov S, Tsurin V, et al. Sedimentation of Fe_3O_4 nanosized magnetic particles in water solution enhanced in a gradient magnetic field. *J Nanopart Res* **14**(3): 740 (2012)

[14] Gong X, West B, Taylor A, Li L. Study on nanometer-thick room-temperature ionic liquids (RTILs) for application as the media lubricant in heat-assisted magnetic recording (HAMR). *Ind Eng Chem Res* **55**(22): 6391–6397 (2016)

[15] Satoshi H, Hamaguchi H. Discovery of a magnetic ionic liquid [bmim]$FeCl_4$. *Chem Lett* **33**(12): 1590–1591 (2004)

[16] Nie L R, Song H, Yohannes A, Liang S W, Yao S. Extraction in cholinium-based magnetic ionic liquid aqueous two-phase system for the determination of berberine hydrochloride in *Rhizoma coptidis*. *RSC Adv* **8**(44): 25201–25209 (2018)

[17] Santos E, Albo J, Irabien A. Magnetic ionic liquids: Synthesis, properties and applications. *RSC Adv* **4**(75): 40008–40018 (2014)

[18] Sajid M. Magnetic ionic liquids in analytical sample preparation: A literature review. *TrAC-Trends Anal Chem* **113**: 210–223 (2019)

[19] Yoshizawa M, Xu W, Angell C A. Ionic liquids by proton transfer: Vapor pressure, conductivity, and the relevance of ΔpK_a from aqueous solutions. *J Am Chem Soc* **125**(50): 15411–15419 (2003)

[20] Okabe T, Moritaka D, Miyatake M, Kondo Y, Sasaki S, Yoshimoto S. Development and performance of a magnetic ionic liquid for use in vacuum-compatible non-contact seals. *Precis Eng* **47**: 97–103 (2017)

[21] Nevshupa R, Conte M, del Campo A, Roman E. Analysis of tribochemical decomposition of two imidazolium ionic liquids on Ti–6Al–4V through mechanically stimulated gas emission spectrometry. *Tribol Int* **102**: 19–27 (2016)

[22] Cowie S, Cooper P K, Atkin R, Li H. Nanotribology of ionic liquids as lubricant additives for alumina surfaces. *J Phys Chem C* **121**(51): 28348–28353 (2017)

[23] Amiril S A S, Rahim E A, Embong Z, Syahrullail S. Tribological investigations on the application of oil-miscible ionic liquids additives in modified Jatropha-based metalworking fluid. *Tribol Int* **120**: 520–534 (2018)

[24] Kim J Y, Kim J T, Song E A, Min Y K, Hamaguchi H O. Polypyrrole nanostructures self-assembled in magnetic ionic liquid as a template. *Macromolecules* **41**(8): 2886–2889 (2008)

[25] Wang H, Yan R Y, Li Z X, Zhang X P, Zhang S J. Fe-containing magnetic ionic liquid as an effective catalyst for the glycolysis of poly(ethylene terephthalate). *Catal Commun* **11**(8): 763–767 (2010)

[26] Sang H L, Ha S H, You C Y, Koo Y M. Recovery of magnetic ionic liquid [bmim]$FeCl_4$ using electromagnet. *Korean J Chem Eng* **24**(3): 436–437 (2007)

[27] Mallick B, Balke B, Felser C, Mudring A V. Dysprosium room-temperature ionic liquids with strong luminescence and response to magnetic fields. *Angew Chem Int Ed* **47**(40): 7635–7638 (2008)

[28] Bombard A J F, Gonçalves F R, Shahrivar K, Ortiz A L, De Vicente J. Tribological behavior of ionic liquid-based magnetorheological fluids in steel and polymeric point contacts. *Tribol Int* **81**: 309–320 (2015)

[29] Shi X, Huang W, Wang X L. Ionic liquids-based magnetic nanofluids as lubricants. *Lubr Sci* **30**(2): 73–82 (2018)

[30] Zhang C L, Zhang S M, Song S Y, Yang G B, Yu L G, Wu Z S, Li X H, Zhang P Y. Preparation and tribological properties of surface-capped copper nanoparticle as a water-based lubricant additive. *Tribol Lett* **54**(1): 25–33 (2014)

[31] Mirjavadi S S, Alipour M, Hamouda A M S, Matin A, Kord S, Afshari B M, Koppad P G. Effect of multi-pass friction stir processing on the microstructure, mechanical and wear properties of AA5083/ZrO_2 nanocomposites. *J Alloys Compd* **726**: 1262–1273 (2017)

[32] Sahoo R R, Math S, Biswas S K. Mechanics of deformation under traction and friction of a micrometric monolithic MoS_2 particle in comparison with those of an agglomerate of nanometric MoS_2 particles. *Tribol Lett* **37**(2): 239–249 (2010)

[33] Liu H T, Cao S F, Ge S R, Jin J. Study on the variation of 3D topography of specific spot on sliding wear surface. *Mater Lett* **65**(23–24): 3512–3515 (2011)

[34] Crist B V. *Handbook of Monochromatic XPS Spectra: The Elements and Native Oxides*. New York (USA): John Wiley and Sons, 2000.

[35] Gao J N, Ran X Z, Shi C M, Cheng H M, Cheng T M, Su Y P. One-step solvothermal synthesis of highly water-soluble, negatively charged superparamagnetic Fe_3O_4 colloidal nanocrystal clusters. *Nanoscale* **5**(15): 7026–7033 (2013)

[36] Schemme T, Pathé N, Niu G, Bertram F, Kuschel T, Kuepper K, Wollschläger J. Magnetic anisotropy related to strain and thickness of ultrathin iron oxide films on MgO(001). *Mater Res Express* **2**(1): 016101 (2015)

[37] Liang S, Zhang G, Min J Z, Ding J Q, Jiang X M. Synthesis and antibacterial testing of silver/poly (ether amide) composite nanofibers with ultralow silver content. *J Nanomater* **2014**: 684251 (2014)

[38] Xue Z P, Gao H, Li X H. A Green and lower-temperature synthesis of two-color fluorescent nitrogen doped graphene quantum dots. *Dyes Pigments* **156**: 379–385 (2018)

[39] Abu-Zied B M, Asiri A M. Synthesis of Dy_2O_3 nanoparticles

via hydroxide precipitation: Effect of calcination temperature. *J Rare Earth* **32**(3): 259–264 (2014)

[40] Jeon S, Hwang H. Effect of hygroscopic nature on the electrical characteristics of lanthanide oxides (Pr_2O_3, Sm_2O_3, Gd_2O_3, and Dy_2O_3). *J Appl Phys* **93**(10): 6393–6395 (2003)

[41] Chen S, Liu W M. Oleic acid capped PbS nanoparticles: Synthesis, characterization and tribological properties. *Mater Chem Phys* **98**(1): 183–189 (2006)

[42] Xiong L P, He Z Y, Xu H, Lu J L, Ren T H, Fu X S. Tribological study of triazine derivatives as additives in rapeseed oil. *Lubr Sci* **23**(1): 33–40 (2011)

[43] Zeng Y W, Ma D K, Wang W, Chen J J, Zhou L, Zheng Y Z, Yu K, Huang S M. N, S co-doped carbon dots with orange luminescence synthesized through polymerization and carbonization reaction of amino acids. *Appl Surf Sci* **342**: 136–143 (2015)

[44] Liang P P, Wu H, Zuo G Z, Ren T H. Tribological performances of heterocyclic-containing ether and/or thioether as additives in the synthetic diester. *Lubr Sci* **21**(3): 111–121 (2009)

[45] Yin W Q, Chen M Q, Lu T H, Akashi M, Huang X H. Properties of complex of Tb(III) and poly(*N*-isopropylacrylamide)-*g*-poly(*N*-isopropylacrylamide-*co*-styrene) core-shell nanoparticles. *J Alloy Compd* **432**(1–2): L18–L21 (2007)

[46] Kingshott P, Thissen H, Griesser H J. Effects of cloud-point grafting, chain length, and density of PEG layers on competitive adsorption of ocular proteins. *Biomaterials* **23**(9): 2043–2056 (2002)

[47] Yamamoto K, Koga Y, Fujiwara S, Kokai F, Kleiman J I, Kim K K. Carbon nitride thin films prepared by nitrogen ion assisted pulsed laser deposition of graphite using KrF excimer laser. *Thin Solid Films* **339**(1–2): 38–43 (1999)

[48] Ma J F, Li C T, Zhao L K, Zhang J, Song J K, Zeng G M, Zhang X N, Xie Y N. Study on removal of elemental mercury from simulated flue gas over activated coke treated by acid. *Appl Surf Sci* **329**: 292–300 (2015)

Jiajia JIA. She received her bachelor degree in 2016 in Nanyang Normal University, China. After then, she is a master graduate student in the Engineering Research Center for Nanomaterials, Henan University, China. Her interests include the design and preparation of novel ionic liquids as lubricant and lubricating additives.

Guangbin YANG. He received his Ph.D. degree in condensed matter physics in 2011 from Henan University, China. Now he is an associate professor at Henan University. His research areas cover the nanotribology, the lubricants, and nano-additives. He has published more than 50 journal papers and possessed two ministerial and provincial-level science and technology awards.

Chunli ZHANG. She received her Ph.D. degree in polymer chemistry and physics in 2013 from Henan University, China. Now she is an associate professor at Henan University, China. Her research interests include the design and preparation of functionalized ionic liquids as lubricant and lubricating additives, nanotribology and nano-additives.

Shengmao ZHANG. He received his Ph.D. degree in physical chemistry from Lanzhou Institute of Chemical Physics of the Chinese Academy of Science in 2004, China. Now he is a professor at Henan University, China. His current research interests include nanoparticle lubricant additives, high performance lubricants and functional materials, and the tribology of materials. He has published more than 90 journal papers and holds 16 Chinese patents.

Yujuan ZHANG. She received her Ph.D. degree in physical chemistry in 2004 from Lanzhou Institute of Chemical Physics of the Chinese Academy of Science, China. Now she is an associate professor at Henan University, China. Her current research interests include nanoparticle lubricant additives, functional materials, and the tribology of materials.

Pingyu ZHANG. He is a professor and the director of the Engineering Research Center for Nanomaterials in Henan University, China. He received his Ph.D. degree from Lanzhou Institute of Chemical Physics, Chinese Academy of Sciences in 2000, China. His current research interests cover nanoparticle lubricant additives, high performance lubricants and functional materials, and the tribology of materials. He has published over 100 journal papers and gained a number of ministerial and provincial-level science and technology awards.